Published in final edited form as:
J Neural Eng. 2013 October ; 10(5): . doi:10.1088/1741-2560/10/5/056013.

Multi-electrode stimulation in somatosensory cortex increases probability of detection

Boubker Zaaimi[1], **Ricardo Ruiz-Torres**[1], **Sara A. Solla**[1,2], and **Lee E Miller**[1,3,4]

Lee E Miller: lm@northwestern.edu

[1]Department of Physiology, Northwestern University, Chicago, IL, 60611, USA

[2]Department of Physics and Astronomy, Northwestern University, Evanston, IL, 60208, USA

[3]Department of Physical Medicine and Rehabilitation, Northwestern University, Chicago, IL, 60611, USA

[4]Department of Biomedical Engineering, Northwestern University, Evanston, IL, 60208, USA

Abstract

Brain machine interfaces (BMIs) that decode control signals from motor cortex have developed tremendously in the past decade, but virtually all rely exclusively on vision to provide feedback. There is now increasing interest in developing an afferent interface to replace natural somatosensation, much as the cochlear implant has done for the sense of hearing. Preliminary experiments toward a somatosensory neuroprosthesis have mostly addressed the sense of touch, but proprioception, the sense of limb position and movement, is also critical for the control of movement. However, proprioceptive areas of cortex lack the precise somatotopy of tactile areas. We showed previously that there is only a weak tendency for neighboring neurons in area 2 to signal similar directions of hand movement. Consequently, stimulation with the relatively large currents used in many studies is likely to activate a rather heterogeneous set of neurons. Here, we have compared the effect of single-electrode stimulation at sub-threshold levels to the effect of stimulating as many as seven electrodes in combination. We found a mean enhancement in the sensitivity to the stimulus (d') of 0.17 for pairs compared to individual electrodes (an increase of roughly 30%), and an increase of 2.5 for groups of seven electrodes (260%). We propose that a proprioceptive interface made up of several hundred electrodes may yield safer, more effective sensation than a BMI using fewer electrodes and larger currents.

Keywords

Monkey; Area 2; intracortical microstimulation

1. Introduction

Efferent BMIs have progressed tremendously since the first demonstrations of 2- and 3-dimensional cursor control in 2002 [1, 2]. However, despite the increased complexity of control, virtually all implementations rely on visual feedback to plan and guide movement. The critical role of proprioception is highlighted by a small group of patients who have lost proprioception yet retain normal muscle strength. These patients make movements that are significantly impoverished compared to normal [3]. There is only a single example that we are aware of, in which proprioceptive feedback was used to augment vision during BMI control [4]. That study used recordings from the primary motor cortex (M1) of a monkey to predict intended hand movement. These movement predictions were used to move not only the cursor, but also the monkey's own limb via a kinarm exoskeleton. When the monkey learned to relax and allowed its arm to be moved passively, several of the metrics used to

evaluate the quality of the BMI guided cursor movements showed improvements over the vision-only condition.

While this natural proprioception demonstration suggests that restoring somatosensation may improve the quality of BMI movement control, it does not offer a practical means of doing so. This limitation needs to be overcome if we are to develop an afferent interface that would complement existing efferent interfaces. Consideration has been given to electrical stimulation applied in the periphery [5–7] as well as in the central nervous system [8–10]. The cochlear implant is a successful example of an afferent interface, by now used to restore hearing in over 200,000 patients in 70 countries [11]. Analogous attempts to use cortical stimulation are much less well developed [12, 13]. For a patient with a complete spinal cord injury, only the central approach would be possible. These and other considerations essential to the development of a somatosensory interface have been reviewed recently [14].

Preliminary experiments toward a somatosensory cortical neuroprosthesis have been carried out by several groups [8, 10, 15–17], although most of these addressed the sense of touch rather than proprioception. A few of these experiments used stimulus trains designed to be biomimetic, including early experiments which demonstrated that monkeys could interpret the frequency of intracortical microstimulation (ICMS) in area 3b much as they interpreted mechanical stimulation of the respective field of their fingertip [10, 17]. In recent experiments, monkeys readily substituted ICMS in either area 3b or area 1 for force of indentation applied to the fingertip [18]. Other experiments have evaluated the monkey's ability to extract useful information from arbitrarily designed stimulus trains meant to replace the sense of touch by stimulating area 1 [9] and proprioception through stimulation near the border of areas 1 and 2 [19].

Because of the considerable redundancy in the motor system, the roughly 100 single neurons that can be recorded with 100 electrodes yield a large amount of movement related information. In contrast, somatosensory stimulation for perception has quite different logistics. It is not possible nor effective to activate single neurons with ICMS; activation of a small number of neurons would be unlikely to reach perceptual threshold, much less yield a robust sensation. Assuming an excitability constant of 1300 $\mu A/cm^2$, stimulation with a 100 μA current will activate neurons within approximately 300 μm of the electrode tip [20, 21]; this region corresponds to a volume of 0.11 mm^3 and includes about 10,000 neurons [22]. Although there is a rough somatotopy in areas 3a and 2, these maps are not as well defined as the corresponding tactile maps in areas 3b and 1. Furthermore, there is only weak tendency for neighboring neurons in area 2 to have similar preferred directions [23]; in that study, pairs of neurons recorded from the same electrode were twice as likely to have PDs aligned within 30 degrees than pairs of neurons recorded from different electrodes, separated by 400 μm or more. Homogeneity in the preferred direction (PD) of activated neurons is thus likely to be increased by using lower stimulation currents. The use of large number of electrodes, each delivering a low current, might be expected to activate a larger number of more nearly homogeneous neurons than could be achieved with higher currents delivered through fewer electrodes. However, there has been very little study of the effect of simultaneous stimulation on multiple electrodes. Investigators have tested several pairs of electrodes chronically implanted in the primary visual cortex of a patient blind for 22 years [24]. Across three such combinations, stimulation of the second electrode reduced the detection threshold of the first by 13%. In a fourth pair there was a 37% change, and no effect in a fifth pair

In this study, we have systematically compared the effect of single-electrode stimulation at sub-threshold levels to the combined effect of as many as 7 electrodes. In nearly 250 experiments in two monkeys, we have found a mean enhancement in stimulus effects of

approximately 30% for pairs of electrodes, and much larger effects for larger groups of electrodes. We suggest that an afferent BMI making use of 5 to 10 μA currents across several hundred or more electrodes may yield safer, more effective activation than larger currents across a small number of electrodes.

2. Methods

2.1. Monkeys

All surgical and experimental procedures were approved by the Institutional Animal Care and Use Committee of Northwestern University. Two male rhesus macaque monkeys (monkey P: 11 Kg and monkey K: 12 Kg) were each implanted with a 1 mm length, 96-electrode, sputtered iridium-oxide microelectrode array (Blackrock Microsystems, Inc) in the proximal arm representation of somatosensory cortical area 2. Area 2 cells receive combined input from both deep muscle receptors and cutaneous receptors. In earlier recordings using the same localization methods, 90% (198/219) of cells responded during active or passive limb movements, very likely due to input both types of receptors [25]. During surgery, we used a combination of M1 stimulation (in both monkeys) and recording of S1 activity during joint rotation and skin stimulation (in monkey K) to localize shoulder and arm receptive fields. We attempted to implant the arrays in this physiologically defined arm area (approximately 1.5 cm from midline), at the caudal most extent of the post-central gyrus.

2.2. Task

Prior to the implant, monkeys were trained to hold the handle of a two-link planar manipulandum used to control a cursor displayed on an LCD screen. Torque motors built into the manipulandum could be used to deliver force pulses to the handle while the cursor was held in a central target. Monkey P was trained in a task that required him to move to a single outer target within a limited time upon sensing a perturbation. These trials started with both center and outer targets displayed, and the monkey had to maintain the cursor in the center target during a random (0.5–5 s) delay period. The perturbation served as the go cue, and the monkey had 1.4 s to hit the outer target and receive a reward. If the monkey moved before the perturbation was delivered, the trial was aborted. Because the chance level performance was not well defined for this task, we chose instead to train Monkey K in a two alternative forced choice task. After holding the cursor in the center target for 0.5 s, the monkey received an audible go cue and two outer targets appeared, one to the right and one to the left of the center target. The monkey moved to the right target if it sensed the perturbation, and to the left if it did not. The monkey received the same reward for successful trials, whether they were true positives (hits) or true negatives.

After each monkey learned its respective task, the force pulse was replaced by ICMS, which was the stimulus used for the experiments reported here. Manipulandum position and force, and ICMS timing were collected using a 128-channel Cerebus data acquisition system (Blackrock Microsystems). Stimuli were randomly delivered and interleaved with 60% no-stimulation trials. A reward was delivered after each successful trial. Typically, fewer than 20% (monkey P) and 15%(monkey K) of the no stimulation trials were false alarms.

2.3. ICMS

ICMS was delivered using the RX7 microstimulator and the MS16 stimulus isolator (Tucker-Davis Technologies, Inc). The stimulus consisted of a train of 120 biphasic pulses at 330 Hz; each phase lasted 200 μs. The current intensity ranged from 0 to 40 μA, selected randomly on each trial. The stimulus was monitored on the oscilloscope; for monkey K the negative phase preceded the positive phase, while for monkey P the negative phase followed

the positive one. To build a psychometric curve, we used 5 different currents spanning a small range above and below the typical threshold currents that had been previously determined for the monkey.

When using multiple electrodes, all were stimulated simultaneously; these trials were randomly intermixed with single electrode and no-stimulation trials. Because of the large number of conditions in the multi-electrode experiments, we needed to determine a single current with which to stimulate each electrode. In monkey P, we computed approximate psychometric curves early in each session. From these curves we chose an appropriate subliminal current (one that yielded approximately 30% normalized response probability) for each electrode. This current, typically ranging from 10 to 35 μA (median = 17.5 μA), was applied to each electrode later in the same session in multi-electrode trials involving from three to seven electrodes. In monkey K, we used the same strategy, although based on psychometric curves computed in previous experimental sessions. For both monkeys, the effect of stimulating several electrodes was always compared to the effect of stimulating individual electrodes in the same session, in randomly intermixed trials. The earliest experiments with monkey K used very small currents (4–7 μA). When thresholds increased about four months post implant, we began using larger currents, ranging from 25 to 37 μA.

2.4. Statistical analysis

To build a stimulus-detection probability map, we first stimulated each electrode individually at 40 μA. We used a χ^2 test to calculate the probability that the monkey's responses were significantly different from those in the absence of stimulation. Among those electrodes that evoked a significant response, we did further tests using a range of smaller currents. For each stimulus current i, we computed the hit rate (HR_i) for the stimulation trials and the false alarm rate (FAR_0) for non-stimulation trials. The sensitivity index d' was then computed from

$$d'(i) = z(HR_i) - z(FAR_0), \quad \text{Eq. 1}$$

where $z(p)$ is the z-score that inverts the cumulative Gaussian distribution.

The index d' characterizes discriminability in signal detection theory [26]. It quantifies the monkey's ability to discriminate presence vs. absence of intracortical stimulation without relying on hypotheses about the criterion used by the monkey to translate percepts into the measured responses.

Next we calculate a detection threshold for each electrode by modeling the probability of response, $P(i) \equiv HR_i$. We note that under no-stimulation, when $i = 0$, there is a non-zero probability of response, $P_0 \equiv FAR_0$. We also note that as the amplitude i of the simulating current is increased, the probability of response saturates at a maximum value P_{max}. In order to track the probability of response due to stimulation, we subtract the baseline and define a normalized probability

$$\overline{P}(i) = \frac{P(i) - P_0}{1 - P_0}. \quad \text{Eq. 2}$$

This normalized probability ranges from $\bar{P}(i = 0) = 0$ to a maximum value

$$\overline{P}_{\max}=\frac{P_{\max}-P_0}{1-P_0}. \quad \text{Eq. 3}$$

We model the probability of response under stimulation as

$$\overline{P}(i)=\overline{P}_{\max}\sum(i,i_{th},\beta), \quad \text{Eq. 4}$$

where $\Sigma(i, i_{th}, \beta)$ is the sigmoidal function

$$\sum(i,i_{th},\sigma)=\left[1+e^{-\beta(i-i_{th})}\right]^{-1}. \quad \text{Eq. 5}$$

The two parameters that characterize the sigmoidal function of Eq. 5, the threshold i_{th} and the slope β, are electrode-specific and follow from the fit of the data to the model of Eq. 4. We thus obtain a threshold value i_{th} for the stimulation current of each electrode.

We note that the model defined by Eqs. 2, 4, and 5, can be rewritten in the standard form for psychometric curves:

$$P(i)=(P_0)+(P_{\max}-P_0)\sum(i,i_{th},\beta), \quad \text{Eq. 6}$$

Of the four parameters in Eq. 6, two are measured - the response rates P_0 and $P_{\max}$ – and two follow from the fit of the data to the model - the parameters i_{th} and β that characterize the sigmoidal function.

To evaluate the interaction amongst electrodes, we compute a theoretical probability of response to the simultaneous stimulation of n electrodes with a current of amplitude i. Under the assumption that the stimulation of each electrode independently affects the probability of response, the theoretically combined, probability of response due to stimulation is $\overline{P_c}(i)$, given by:

$$\overline{P}_c(i)=1-\left[\left(1-\overline{P}_1(i)\right)\left(1-\overline{P}_2(i)\right)\ldots\left(1-\overline{P}_n(i)\right)\right]. \quad \text{Eq. 7}$$

The combined effect of multi-electrode stimulation on the sensitivity index d' can also be estimated under the independence assumption. The value of $d'_c(i)$ follows from Eq. 1:

$$d'_c(i)=z\left(P_c(i)\right)-z(P_0). \quad \text{Eq. 8}$$

As before, $FAR_0 = P_0$ is the rate of spontaneous response under no stimulation. Under simultaneous stimulation of n electrodes with a current of amplitude i, $HR_i = P_c(i)$ is the total probability of response, which follows from inverting Eq. 2, namely $P_c(i) = P_{\bar{c}}(i) + P_0(1 - P_{\bar{c}}(i))$, with $\overline{P_c}(i)$ estimated under the independence assumption as per Eq. 7.

3. Results

3.1. Detection of single-electrode ICMS in somatosensory area 2

We conducted a total of 249 stimulation experiments in two monkeys (P and K) over the course of 25 weeks. Experiments with monkey P were begun nearly a year after the array

was implanted, following a series of recording experiments. In contrast, stimulation experiments began two weeks following implant in monkey K.

We initially mapped both the arrays in a series of 10–12 sessions using 120 biphasic pulses at a fixed 40 μA stimulus current. We concentrated subsequent experiments on those electrodes that elicited a behavioral response to stimulus significantly different from the behavior observed on randomly interleaved no-stimulus trials (χ^2 test; $p < 0.05$). By this criterion, we selected 21 of the 95 electrodes for monkey P (figure 1(b)) and 87 electrodes for monkey K (figure 1(d)). Fourteen of the 21 (67%) electrodes for monkey P were located in the anterolateral quadrant of the array.

The much larger percentage of effective electrodes for monkey K may have been due to the short time between implant and stimulation experiments. After 15 weeks, experiments with monkey K were suspended for three weeks. During this interval, many of the electrodes became significantly less responsive, for unknown reasons. As a result, we split the data from monkey K into two datasets K_E (early data) and K_L (later data). After the three-week interruption, we selected 43 random electrodes to be retested at 40 μA. At this point, only 12 of the 43 (28%) had scores significantly different from the no-stimulation condition. These electrodes were located mainly in the posterior half of the array, and their scores are represented below the diagonal of each square in figure 1(d). Electrodes marked with an “x” were not retested.

In order to characterize the effect of stimulation more completely, we constructed psychometric curves describing the probability of detection as a function of the stimulus current. Figure 2(a) shows an example of a stimulus detection experiment using a single electrode (monkey K). In this session, 31 of 182 no-stimulation trials (17%) were false alarms, in which the monkey incorrectly responded as though there had been a stimulus. At 8 μA, the monkey responded positively in 7 out of 19 trials (37%), a level that was significantly different from the no-stimulation condition (χ^2 test; $p < 0.05$). For currents at or above 12 μA, the monkey reported detecting the stimuli virtually every time. A sigmoidal fit to the normalized scores yielded a threshold at 9 μA.

We computed psychometric curves for 21 electrodes for monkey P; 67% had a threshold below 25 μA (figure 2(b)). The modal threshold was below 20 μA. Psychometric curves for early experiments with monkey K had much lower thresholds: among 10 tested electrodes, four had thresholds below 5 μA and three had thresholds between 5 and 10 μA (blue bars in figure 2(c)). After the three-week interruption, thresholds rose above 10 μA in six of seven electrodes (red bars in figure 2(c)). The average threshold across all experiments for both monkeys was 26 μA.

3.2. Simultaneous stimulation of two electrodes

In order to evoke something like the natural pattern of activity occurring in the cortex when the limb is perturbed, we would expect to need to stimulate across a very large number of electrodes simultaneously. For this reason, it is of great interest to know how the effect of stimulation sums across electrodes. We tested this effect in 95 pairs of electrodes, stimulating each electrode in the pair both individually and together, using subthreshold currents based on each electrode’s psychometric curve (figure 3).

To quantify the effect of simultaneous stimulation, we converted all response scores to d' measures. We represented the increased likelihood of stimulus detection in terms of the change in d' ($\Delta d'$) due to the simultaneous stimulation of both electrodes relative to the larger of the two d' measures for the individual electrodes:

$$\Delta d' = d'_{1,2} - \max(d'_1, d'_2) \quad \text{Eq. 9}$$

For both monkeys, paired stimulation had significantly greater effect than the most effective individually stimulated electrode (figure 3c). The distribution of $\Delta d'$ was unimodal for both monkeys (AIC: monkey P unimodal=52, bimodal=53; monkey K unimodal=86, bimodal=90). The mean increase in d' across all pairs was 0.17±0.5, which was significantly greater than 0 (t-test p=0.0009). The mean increase for monkey P was 0.14±0.4 (t-test p=0.02). The mean $\Delta d'$ for monkey K was larger for dataset K_E (0.35±0.3) than for K_L (0.13 ±0.6), and was significant only for K_E (t-test p=0.009). For dataset K_E, only 25% of the electrode pairs yielded detection at significantly higher levels than the individual electrodes (Fisher test, $p < 0.05$), in part, probably because of the small numbers of repeated trials for a given condition. None of the negative $\Delta d'$ was significant for any of the datasets. On average, the probability of response to stimulation measured when stimulating 2 electrodes did not differ significantly from the theoretical $\bar{P_c}$ obtained in Eq. 7 under the independence assumption (monkey K: $\bar{P_c}$ = 0.48±0.27, actual score = 0.47±0.25, paired t-test = 0.44; monkey P: $\bar{P_c}$ = 0.82±0.24, actual score = 0.81 ±0.23, paired t-test = 0.29).

There was a weak, negative correlation R between the maximum d' of the individual electrodes in the pair and $\Delta d'$ for the pair: R = −0.14 for monkey K and R = −0.28 for monkey P. Thus, $\Delta d'$ tended to be somewhat lower for pairs that included a more effective individual electrode. This correlation was significant only for monkey P (p=0.047). There was however, no correlation between electrode spacing and $\Delta d'$, nor was there a significant difference in $\Delta d'$ between the 43 electrode pairs separated by less than 800 μm and the 50 electrode pairs separated by more than 800 μm (t-test and rank sum test p>0.1).

3.3. Simultaneous stimulation of multiple electrodes

Further increases in $\Delta d'$ were observed for both monkeys when more than two electrodes were stimulated simultaneously. These experiments required the determination of sub-threshold currents for as many as seven electrodes; these subliminal currents were later applied both to the individual electrode and to combinations of electrodes. Several typical experiments are shown in figure 4, both for monkey P (top) and monkey K (bottom). For monkey P, 92% of the groups of simultaneously activated electrodes were more effective than the single most effective electrode in the group. For monkey K, the corresponding number was 78% ($\chi^2 < 0.05$).

Not only did $\Delta d'$ become larger when larger numbers of electrodes were stimulated, the actual probability of response to stimulation was significantly higher, on average, than the theoretical $\bar{P_c}$ obtained in Eq. 7 under the independence assumption (blue lines in figure 4). For each dataset, combining all cases with more than two stimulated electrodes, the actual normalized response $\bar{P}$ was larger than the theoretical combined response $\bar{P_c}$ (monkey K: $\bar{P}$ = 0.73±0.22, $\bar{P_c}$ = 0.56±0.25, paired t-test = 0.01; monkey P: $\bar{P}$ = 0.87 ± 0.21, $\bar{P_c}$ = 0.51±0.16, paired t-test = 0.51e-05). This suggests that there was a nonlinear, facilitatory effect of the combined stimulation.

We computed the increase in detection sensitivity for groups of 2–7 electrodes, and discovered that sensitivity increased progressively with the number of electrodes for both monkeys (figure 5). A line was fitted to this data; its slope was positive and significantly different from zero for both monkeys (monkey P: $R^2 = 0.68$, t-test of slope = 10^{-7}; monkey K: $R^2 = 0.26$, t-test of slope = 0.008). In experiments in which seven electrodes were simultaneously stimulated (monkey P), d' increased by 2.46, a 260% increase relative to its value when only the single best electrode was stimulated.

4. Discussion

4.1. Summary of results

In a series of experiments with two monkeys we have demonstrated that the monkey's ability to detect trains of electrical stimulation delivered to area 2 of the primary somatosensory cortex scales roughly with the number of electrodes. This scaling allowed the monkeys to reliably detect stimulation currents that were well below the level of detection of individual electrodes. This potentiation effect increased as the effectiveness of any individual electrode grew smaller, but was apparently not dependent on the spatial separation between electrodes. The use of lower currents on individual electrodes has several important implications, including the ability to implement the activation of a more homogeneous group of neurons, and to reduce tissue and electrode damage.

4.2. Effective radius of activation

The volume of tissue activated by ICMS is determined in large part by the magnitude of the stimulus current and the excitability of the neuronal elements being stimulated. The latter is characterized by the tissue excitability constant K, defined as the current necessary for a 200 μs cathodal pulse to evoke a spike from a neuron 1 mm from the electrode tip with 50% probability. The effective current spread is equal to the square root of the current divided by the square root of K [20]. The excitability constant K varies greatly, ranging from 300 μA/mm^2 for large myelinated axons to 27000 μA/mm^2 for small unmyelinated cortical neurons [21, 27]. For pyramidal neurons in cat motor cortex, K is approximately 1300 μA/mm^2 [21]. The excitability constant in area 2 is likely to be somewhat larger than that of M1, perhaps 2000 μA/mm^2. Therefore, in our experiments, for a stimulus of 40 μA and pulse width of 200 μs, the effect of the current might extend 150 μm from the electrode tip.

Current spread can also be investigated using behavioral methods. Murasugi et al stimulated area MT of monkeys in an attempt to activate these visually sensitive neurons and thus bias the monkeys' discrimination of the direction of motion of partially coherent dots. Stimulation with 1s trains of 200 Hz, 200 μs pulses was often successful, provided that the current was less than 20 μA. Higher currents presumably spread beyond the 100 μm radius of a single directional column, causing a non-uniform perceptual effect [28, 29]. Similar conclusions were drawn from experiments with blind human patients who received ICMS through electrodes chronically implanted in V1 [24]. With threshold currents mostly below 25 μA, 34 of 38 electrodes produced small, circular phosphenes that were generally colored. As the current was increased, the phosphenes typically became white, greyish or yellowish, possibly due to the activation of increasingly heterogeneous groups of cells. V1 microstimulation has also been used to delay visually guided saccades in monkeys [30, 31]. These experiments imply that 100 μs, 200 Hz trains of 200 μs pulses spread 280 μm from the electrode tip for currents of 50 μA.

4.3 Use of multiple electrodes to deliver increased stimulus effectiveness

Cells in area 2 have approximately sinusoidal tuning curves with respect to the direction of hand movement [32]. We have shown previously that the preferred directions (PDs) of area 2 neurons recorded from the same electrode are more nearly aligned than those of neurons recorded from adjacent electrodes separated by 400 μm [23]. We found no greater PD uniformity for neurons recorded with 400 μm separation than 800 μm. Electrical stimulation that activates a more homogeneous group of closely spaced neurons might be expected to elicit a more nearly coherent percept than stimulation that spreads over larger distances.

In our study, the average single-electrode current necessary to reach detection threshold was 26 μA, a current that might be expected to excite neurons within a 100 μm radius. However,

this average threshold does not include the large number of electrodes that failed to reach threshold at 40 μA and were not tested further. At 40 μA, stimulation probably activated neurons as far as 200 to 300 μm from the electrode tip, near the distance at which PDs no longer tend to cluster [23]. Use of even higher currents to elicit more robust above-threshold effects, could well lead to a loss of specificity as noted above for visual system neurons, thereby yielding less effective perceptual effects. Stimulation across a very large array of electrodes, each with threshold or subthreshold currents, might be expected to generate a much more realistic percept than suprathreshold currents applied to only one or a small number of electrodes.

4.4. Use of multiple electrodes to reduce tissue and electrode damage

In addition to providing a more natural stimulus-driven perception, the use of multiple electrodes and lower currents is also likely to lead to less damage to both the electrodes themselves and the surrounding tissue. Beyond the trauma caused by the array insertion during surgery and the consequences of the bio-incompatibility of the electrode, stimulation can generate toxicity [33] and changes in both intracellular and extracellular ionic concentrations [34].

The amounts of charge/phase and charge density have a synergistic effect, such that greater total charge can lead to electrode damage with smaller charge density. For the sputtered iridium oxide electrode film arrays that we used, the damage threshold using 50 Hz trains and 100 μs pulse width occurred at either a combination of 60 nC charge and 1.9 mC/cm^2 charge density, or 80 nC charge and a charge density of 1.0 mC/cm^2 [35]. The mean detection threshold current of 26 μA in our experiments corresponds to only 5 nC/phase and 0.25 mC/cm^2 charge density, well below the level expected to cause damage to the electrodes. The threshold for tissue damage using SIROF electrodes is somewhat lower than that for electrode damage, but still well above the levels of charge and charge density used in our study [35].

Several studies have shown that stimulation causes acute decreases in electrode impedance. These changes largely recover between sessions, suggesting a reversible electrochemical reaction rather than cumulative damage [36, 37]. In one of these experiments, investigators tracked impedance changes over 200 days and found no difference between electrodes receiving intermittent stimulation at 15 to 30 μA and those receiving no stimulation [37]. Neither study found any deleterious effect of stimulation on the ability to record action potentials. Indeed, there is some evidence that the acute effects of stimulation may actually improve recording quality [36].

The low stimulus currents proposed here appear to be relatively safe with respect to both tissue and electrode damage. However, given the much longer periods of stimulation that might be encountered in actual clinical applications, some caution would still be warranted. Cell loss occurred following 30 days of continuous stimulation at 4 nC/ph and 50 Hz for 8 hours/day [38]. Fortunately, continuous stimulation at 50 Hz is likely to be much higher than a typical application would require. At 50% duty cycle (1 s on, 1 s off), the radial extent of damage decreased from 150 to 60 μm, a level that was nearly the same as that of the unstimulated electrodes. Anecdotal observation was made in one study of seizures caused by concurrent stimulation of 72 electrodes in primary motor cortex at 25 μA [37]. Any stimulus regimen must be far below the level that might induce seizure activity, a precaution that may necessitate currents no higher than 5–10 μA. Here we report behavioral effects due to the simultaneous activation of electrodes. The enhanced detection achieved with very low levels of activation of the individual electrodes is an encouraging and promising result.

Acknowledgments

This work was supported in part by Grant NS-048845 from the National Institute of Neurological Disorders and Stroke, and the Defense Advanced Research Projects Agency under Contract No. N66001-10-C-4056. Further support was provided by the Chicago Community Trust through the Searle Program for Neurological Restoration. We also gratefully acknowledge Dr. Sliman Bensmaia for helpful discussions about stimulus and analytical methods.

References

1. Serruya MD, Hatsopoulos NG, Paninski L, Fellows MR, Donoghue JP. Instant neural control of a movement signal. Nature. 2002; 416:141–2. [PubMed: 11894084]
2. Taylor DM, Tillery SI, Schwartz AB. Direct cortical control of 3D neuroprosthetic devices. Science. 2002; 296:1829–32. [PubMed: 12052948]
3. Sainburg RL, Poizner H, Ghez C. Loss of proprioception produces deficits in interjoint coordination. Journal of neurophysiology. 1993; 70:2136–47. [PubMed: 8294975]
4. Suminski AJ, Tkach DC, Fagg AH, Hatsopoulos NG. Incorporating feedback from multiple sensory modalities enhances brain-machine interface control. J Neurosci. 2010; 30:16777–87. [PubMed: 21159949]
5. Dhillon GS, Horch KW. Direct neural sensory feedback and control of a prosthetic arm. IEEE Trans Neural Syst Rehabil Eng. 2005; 13:468–72. [PubMed: 16425828]
6. Ochoa J, Torebjork E. Sensations evoked by intraneural microstimulation of single mechanoreceptor units innervating the human hand. The Journal of physiology. 1983; 342:633–54. [PubMed: 6631752]
7. Hokanson, JA.; Ayers, CA.; Gaunt, RA.; Bruns, TM.; Weber, DJ. Effects of spatial and temporal parameters of primary afferent microstimulation on neural responses evoked in primary somatosensory cortex of an anesthetized cat. Engineering in Medicine and Biology Society, EMBC, 2011 Annual International Conference of the IEEE; 2011. p. 7533-6.
8. London BM, Jordan LR, Jackson CR, Miller LE. Electrical stimulation of the proprioceptive cortex (area 3a) used to instruct a behaving monkey. IEEE Trans Neural Syst Rehabil Eng. 2008; 16:32–6. [PubMed: 18303803]
9. O'Doherty JE, Lebedev MA, Ifft PJ, Zhuang KZ, Shokur S, Bleuler H, Nicolelis MAL. Active tactile exploration using a brain-machine-brain interface. Nature. 2011; 479:228–31. [PubMed: 21976021]
10. Romo R, Hernandez A, Zainos A, Salinas E. Somatosensory discrimination based on cortical microstimulation. Nature. 1998; 392:387–90. [PubMed: 9537321]
11. NIDCD. Cochler implants. 2011.
12. Wang J, Liu Y, Qin L, Chimoto S, Nakamoto K, Sato Y. Chronic microstimulation of cat auditory cortex effective to evoke detection behaviors. Neuroscience. 2012; 206:81–8. [PubMed: 22285311]
13. Otto KJ, Rousche PJ, Kipke DR. Microstimulation in auditory cortex provides a substrate for detailed behaviors. Hear Res. 2005; 210:112–7. [PubMed: 16209915]
14. Weber DJ, Friesen R, Miller LE. Interfacing the somatosensory system to restore touch and proprioception: Essential considerations. Journal of Motor Behavior. 2012; 44:403–18. [PubMed: 23237464]
15. O'Doherty JE, Lebedev MA, Hanson TL, Fitzsimmons NA, Nicolelis MA. A brain-machine interface instructed by direct intracortical microstimulation. Front Integr Neurosci. 2009; 3:1–10. [PubMed: 19225578]
16. Venkatraman S, Carmena JM. Active sensing of target location encoded by cortical microstimulation. Neural Systems and Rehabilitation Engineering, IEEE Transactions on. 2011; 19:317–24.
17. Romo R, Hernandez A, Zainos A, Brody CD, Lemus L. Sensing without touching: psychophysical performance based on cortical microstimulation. Neuron. 2000; 26:273–8. [PubMed: 10798410]
18. Berg J, Dammann J, Tenore F, Tabot G, Boback J, Manfredi L, Peterson M, Katyal K, Johannes M, Makhlin A, Wilcox R, Franklin R, Vogelstein R, Hatsopoulos N, Bensmaia S. Behavioral

demonstration of a somatosensory neuroprosthesis. IEEE Transactions on Neural Systems and Rehabilitation Engineering. 2013; 21:500–507. [PubMed: 23475375]

19. Dadarlat, MC.; O'Doherty, JE.; Sabes, PN. Annual meeting, Society for Neuroscience. New Orleans: Society for Neuroscience; 2012. Multisensory integration of vision and intracortical microstimulation for sensory substitution and augmentation; p. 292.12
20. Tehovnik EJ, Tolias AS, Sultan F, Slocum WM, Logothetis NK. Direct and indirect activation of cortical neurons by electrical microstimulation. Journal of neurophysiology. 2006; 96:512–21. [PubMed: 16835359]
21. Stoney SD Jr, Thompson WD, Asanuma H. Excitation of pyramidal tract cells by intracortical microstimulation: effective extent of stimulating current. Journal of neurophysiology. 1968; 31:659–69. [PubMed: 5711137]
22. Karlsen AS, Pakkenberg B. Total numbers of neurons and glial cells in cortex and basal ganglia of aged brains with Down syndrome--a stereological study. Cereb Cortex. 2011; 21:2519–24. [PubMed: 21427166]
23. Weber DJ, London BM, Hokanson JA, Ayers CA, Gaunt RA, Ruiz-Torres R, Zaaimi B, Miller LE. Limb-state information encoded by peripheral and central somatosensory neurons: Implications for an afferent interface. Neural Systems and Rehabilitation Engineering, IEEE Transactions on. 2011; 19:501–13.
24. Schmidt E, Bak M, Hambrecht F, Kufta C, O'Rourke D, Vallabhanath P. Feasibility of a visual prosthesis for the blind based on intracortical microsimulation of the visual cortex. Brain. 1996; 119:507–22. [PubMed: 8800945]
25. London BM, Miller LE. Responses of somatosensory area 2 neurons to actively and passively generated limb movements. Journal of neurophysiology. 2013; 109:1505–13. [PubMed: 23274308]
26. Egan, JP. Signal detection theory and ROC analysis. Academic Press; New York: 1975.
27. Nowak LG, Bullier J. Spread of stimulating current in the cortical grey matter of rat visual cortex studied on a new in vitro slice preparation. Journal of neuroscience methods. 1996; 67:237–48. [PubMed: 8872891]
28. Murasugi C, Salzman C, Newsome W. Microstimulation in visual area mt: Effetcts of varying pulse amplitude and frequency. J Neuroscience. 1993; 13:1719–29.
29. Albright TD, Desimone R, Gross CG. Columnar organization of directionally selective cells in visual area MT of the macaque. Journal of neurophysiology. 1984; 51:16–31. [PubMed: 6693933]
30. Tehovnik EJ, Slocum WM, Schiller PH. Microstimulation of V1 delays the execution of visually guided saccades. The European journal of neuroscience. 2004; 20:264–72. [PubMed: 15245498]
31. Tehovnik EJ, Slocum WM, Carvey CE, Schiller PH. Phosphene induction and the generation of saccadic eye movements by striate cortex. Journal of neurophysiology. 2005; 93:1–19. [PubMed: 15371496]
32. Prud'homme MJL, Kalaska JF. Proprioceptive activity in primate primary somatosensory cortex during active arm reaching movements. J Neurophysiol. 1994; 72:2280–301. [PubMed: 7884459]
33. Morton SL, Daroux ML, Mortimer JT. The role of oxygen reduction in electrical stimulation of neural tissue. Journal of The Electrochemical Society. 1994; 141:122–30.
34. McCreery DB, Agnew WF, Yuen TGH, Bullara L. Charge density and charge per phase as cofactors in neural injury induced by electrical stimulation. Biomedical Engineering, IEEE Transactions on. 1990; 37:996–1001.
35. Negi S, Bhandari R, Rieth L, Van Wagenen R, Solzbacher F. Neural electrode degradation from continuous electrical stimulation: Comparison of sputtered and activated iridium oxide. Journal of neuroscience methods. 2010; 186:8–17. [PubMed: 19878693]
36. Otto KJ, Johnson MD, Kipke DR. Voltage pulses change neural interface properties and improve unit recordings with chronically implanted microelectrodes. Biomedical Engineering, IEEE Transactions on. 2006; 53:333–40.
37. Parker, RA.; Davis, TS.; House, PA.; Normann, RA.; Greger, B. Progress in Brain Research. Schouenborg, J., et al., editors. Elsevier; 2011. p. 145-65.

38. McCreery D, Pikov V, Troyk P. Neuronal loss due to prolonged controlled-current stimulation with chronically implanted microelectrodes in the cat cerebral cortex. Journal of neural engineering. 2010; 7:036005. [PubMed: 20460692]

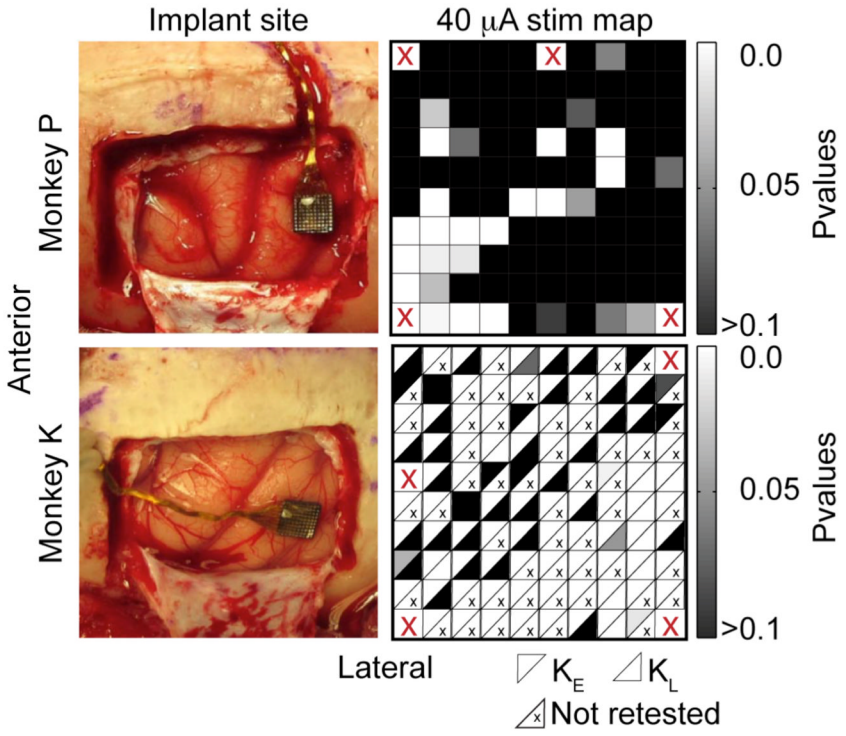

Figure 1.
Cortical implant sites and electrode selection. The left column shows photographs of the implant sites for monkeys P and K, located just anterior of the intraparietal sulcus. The right column shows the significance of the effect of single electrode stimulation at 40 μA (χ^2 test, stim/no-stim trials). The cells in the maps for monkey K indicate values recorded early (K_E, above diagonal) and late (K_L, below diagonal). Electrodes not retested are marked with a small “x”. Four electrodes in each array that were not connected are marked with a red “X”.

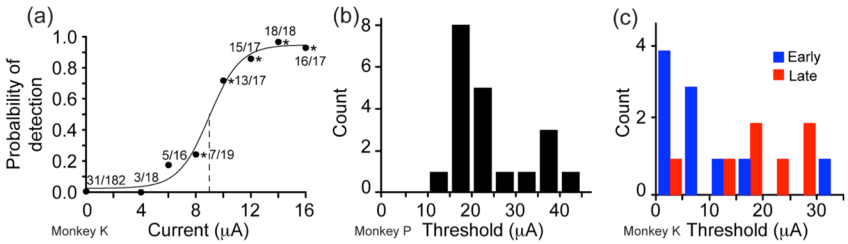

Figure 2.

Single-electrode threshold experiments. (a) Probability of stimulus detection is plotted as a function of stimulus current (monkey K). The numbers along the curve indicate the number of times the monkey reported detection (numerator) and the total number of trials at that current (denominator). There were 31 out of 182 false alarms (no stimulation, 0 current), and nearly 100% hit rate for currents above 10 μA. Threshold (50% response rate) for this electrode was 9 μA. The data were normalized and fitted with a sigmoid as described in the methods. (b) Distribution of detection threshold for all tested electrodes for monkey P. This includes only those electrodes with a significant response at 40 μA. (c) Thresholds for monkey K, including those in the early data set K_E (blue) and those retested in the later dataset K_L (red).

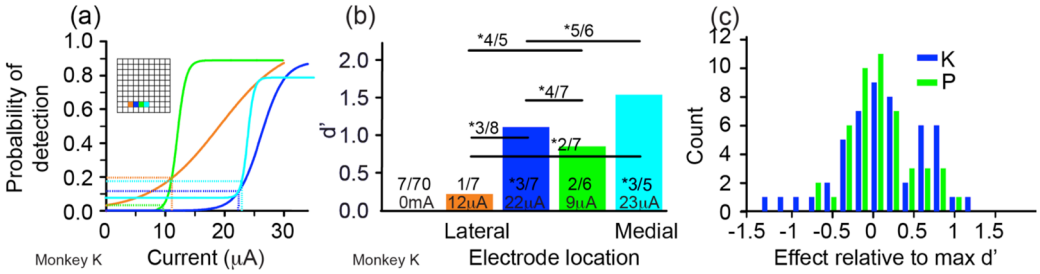

Figure 3.

Change in the probability of detection with paired-electrode stimulation. (a) Sigmoid response curves for 4 different electrodes tested individually within a single session. Inset shows electrode locations. Subthreshold currents were identified for each electrode (vertical colored lines). (b) Later in the same session, these subthreshold currents were used both for single-electrode and paired-electrode stimulation. The colored bars and associated numbers represent the responses for individual electrodes as in 3(a). Numbers above the horizontal lines indicate the responses for the corresponding pair. The "*" indicates significant detection. Paired- and single-electrode stimulation were intermixed during the session. (c) d' scores for all single and paired stimulation conditions in 3(b). This distribution shows the difference $\Delta d'$ between the d' for paired simulation and the larger of the two individual d' scores.

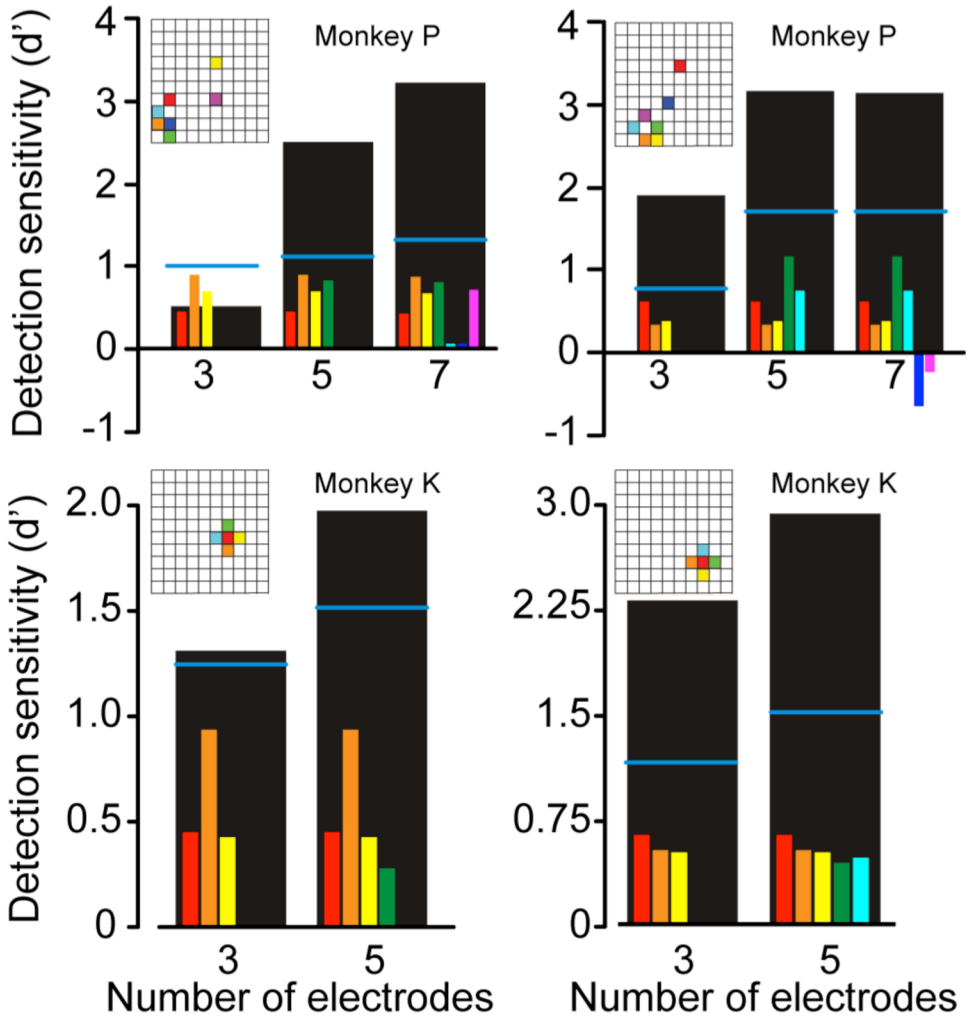

Figure 4.

Increased detection sensitivity $\Delta d'$ with multi-electrode stimulation in four different sessions. The small colored bars in each panel indicate the d' score for each individual electrode when stimulated with a subliminal current. Horizontal blue lines indicate the theoretical score under combined stimulation, d'_c, computed under the independence assumption as per Eq. 8. Large black bars indicate the actual effect of simultaneous stimulation, which exceeded d'_c in 9 out of 10 cases. Insets indicate the location of individual electrodes.

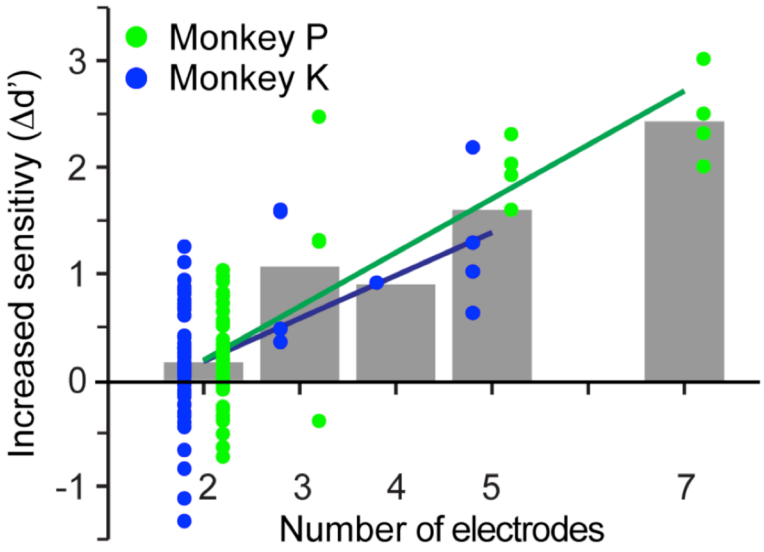

Figure 5.

Relation between the increase $\Delta d'$ in detection sensitivity and the number of stimulated electrodes. Symbols indicate the increase in d' for groups of electrodes of different sizes, measured with respect to the maximum value of d' among those obtained for individual stimulation of each electrode in the group. $\Delta d'$ increased significantly with electrode number for both monkeys.